

See discussions, stats, and author profiles for this publication at: <https://www.researchgate.net/publication/232941598>

A virtual structure approach to formation control of unicycle mobile robots using mutual coupling

Article in *International Journal of Control* · November 2011

DOI: 10.1080/00207179.2011.627686

CITATIONS

62

READS

490

6 authors, including:



[Anna Sadowska](#)

Delft University of Technology

18 PUBLICATIONS 209 CITATIONS

[SEE PROFILE](#)



[Henri Huijberts](#)

Queen Mary, University of London

75 PUBLICATIONS 1,015 CITATIONS

[SEE PROFILE](#)



[Dragan Kostic](#)

ASM Pacific Technology

57 PUBLICATIONS 668 CITATIONS

[SEE PROFILE](#)



[Henk Nijmeijer](#)

Eindhoven University of Technology

936 PUBLICATIONS 22,139 CITATIONS

[SEE PROFILE](#)

Some of the authors of this publication are also working on these related projects:



Cooperative automated maneuvering [View project](#)



Ship control [View project](#)

A virtual structure approach to formation control of unicycle mobile robots using mutual coupling

Anna Sadowska^{a*}, Thijs van den Broek^b, Henri Huijberts^a, Nathan van de Wouw^c,
Dragan Kostić^c and Henk Nijmeijer^c

^aSchool of Engineering and Materials Science, Queen Mary University of London, Mile End Road, E1 4NS London, UK;

^bAutomotive-Integrated Safety, TNO, P.O. Box 756, 5700 AT Helmond, The Netherlands; ^cDepartment of Mechanical Engineering, Eindhoven University of Technology, P.O. Box 513, 5600 MB Eindhoven, The Netherlands

(Received 10 May 2010; final version received 24 September 2011)

In this article, the formation control problem for unicycle mobile robots is studied. A distributed virtual structure control strategy with mutual coupling between the robots is proposed. The rationale behind the introduction of the coupling terms is the fact that these introduce additional robustness of the formation with respect to perturbations as compared to typical leader–follower approaches. The applicability of the proposed approach is shown in simulations and experiments with a group of wirelessly controlled mobile robots.

Keywords: cooperative control; robotics; stability of non-linear systems

1. Introduction

In this article, the formation control problem for unicycle mobile robots is considered. Formation control problems arise when groups of mobile robots are employed to jointly perform certain tasks. The benefits of exploiting groups of robots, as opposed to a single robot or a human, become apparent when considering spatially distributed tasks, dangerous tasks, tasks which require redundancy, tasks that scale up or down in time or tasks that require flexibility. Various areas of application of cooperative mobile robots are e.g. simultaneous localisation and mapping (Durrant-Whyte and Bailey 2006), automated highway systems (Bishop 2005), payload transportation (Wang, Takano, Hirata, and Kosuge 2007), RoboCup (Kitano et al. 1997), enclosing an invader (Yamaguchi 1999) and the exploration of an unknown environment (Burgard, Moors, Stachniss, and Schneider 2005). More examples as well as some background information concerning formation control of mobile robots can be found in Arai, Pagello, and Parker (2002), Chen and Wang (2005) and Parker (2008). Furthermore, in Kolmanovsky and McClamroch (1995) and Morin and Samson (2008) an overview regarding the control of nonholonomic unicycle mobile robots is presented.

Before a wide application of cooperative mobile robotics will become feasible, many technical and scientific challenges must be faced such as the development of cooperative and formation control

strategies, control schemes robust to communication constraints and imperfections, the localisation of the robot position and sensing and environment mapping. In this article, the focus is on the aspect of cooperative control. In the recent literature, see e.g. Beard, Lawton, and Hadaegh (2000), Carelli, de la Cruz, and Roberti (2006), Consolini, Morbidi, Prattichizzo, and Tosques (2006), Do and Pan (2007) and Takahashi, Nishi, and Ohnishi (2004), three different approaches towards the cooperative control of mobile robots are described: the behaviour-based approach, the leader–follower approach and the virtual structure approach. In the behaviour-based approach, a so-called behaviour (e.g. obstacle avoidance, target seeking) is assigned to each individual robot (Arkin 1998). This approach can be naturally used to design control strategies for robots with multiple competing objectives. Moreover, it is suitable for large groups of robots, since it is typically a decentralised strategy. A disadvantage is that the complexity of the dynamics of the group of robots does not lend itself to straightforward mathematical stability analysis. Therefore, to simplify the analysis, the dynamics of individual robots are commonly assumed to be described by a single integrator. Clearly, even kinematic models of nonholonomic mobile robots are more complex, limiting the applicability of this approach in practice.

In the leader–follower approach some robots will take the role of leaders and aim to track predefined trajectories, while the follower robots will follow the

*Corresponding author. Email: a.d.sadowska@qmul.ac.uk

leaders according to a relative posture (Yanakiev and Kanellakopoulos 1996; Desai, Ostrowski, and Kumar 2001; Leonard and Fiorelli 2001; Bicho and Monteiro 2003; Vidal, Shakernia, and Sastry 2003; Tanner, Pappas, and Kumar 2004; Carelli et al. 2006; Consolini et al. 2006; Ikeda, Jongusuk, Ikeda, and Mita 2006). An advantage of this approach is the fact that it is relatively easy to understand and implement. A disadvantage, however, is the fact that there is no feedback from the followers to the leaders. Consequently, if a follower is being perturbed, the formation cannot be maintained and thus such a formation control strategy lacks robustness in the face of such perturbations.

A third approach in cooperative control is the virtual structure approach, in which the robots' formation no longer consists of leaders and followers, i.e. no hierarchy exists in the formation. This approach was studied in e.g. Lewis and Tan (1997), where a general controller strategy is developed for the virtual structure approach. However, using this strategy, it is not possible to consider formations which are time-varying. Moreover, the priority of the mobile robots, either to follow their individual trajectories or to maintain the groups formation, cannot be changed. In Do and Pan (2007), a virtual structure controller is designed for a group of unicycle mobile robots using models involving the dynamics of the robots. Consequently, the controller design tends to be rather complex, which is unfavourable from an implementation perspective, especially when kinematic models suffice. A virtual structure approach towards solving the consensus problem with time-invariant formations for unicycle mobile robots has been proposed in Yoshioka and Namerikawa (2008). As we will show in this article and was also advocated in Young, Beard, and Kelsey (2001), an advantage of the virtual structure approach is that it allows to attain a certain robustness of the formation to perturbations on the robots.

In this article, we consider a formation control problem in which the robots are required to form a desired, possibly time-varying, formation shape and follow a given desired trajectory, as a whole. In this scope, our contributions can be summarised as follows. Firstly, a virtual structure controller is designed for the formation control of a group of nonholonomic unicycle mobile robots, which is based on the kinematics of unicycle mobile robots. This controller contains so-called mutual coupling terms between the robots to ensure robustness of the formation with respect to perturbations. In the face of perturbations, these mutual coupling terms allow the controller to mediate between ensuring tracking of the individual desired trajectories of the robots and

keeping formation. Secondly, the strength of the controller that we propose is the fact that it is distributed; that is, each robot only exchanges information with their neighbours in lieu of a whole formation. Thirdly, we prove the global exponential stability of the formation error dynamics, which is particularly favourable since it provides a certain level of robustness. Fourthly, we extend our main result to a dynamic control algorithm that uses robots' dynamic model as opposed to merely kinematic model considered before. Hence, in this control algorithm robots' dynamic properties such as mass or moment of inertia are taken into consideration. Finally, the control design is validated in simulations and experiments.

This article is organised as follows. In Section 2, preliminary technical results needed in the remainder of this article are presented. The virtual structure control design and a stability proof for the formation error dynamics are given in Section 3. Further, in Section 4 we present simulation results to validate the proposed approach and in Section 5, experimental results are given. Section 6 presents our concluding remarks.

2. Preliminaries

In this section we present some mathematical tools that are employed in further parts of this article.

Definition 2.1 (Lefeber 2000), (cf. Ioannou and Sun 1995; Khalil 1996; Narendra and Annaswamy 1989): A continuous function $\omega: \mathbb{R}^+ \rightarrow \mathbb{R}$ is said to be persistently exciting (PE) if $\omega(t)$ is bounded, Lipschitz, and constants $\delta_c > 0$ and $\epsilon > 0$ exist such that

$$\forall t \geq 0, \exists s : t - \delta_c \leq s \leq t \text{ such that } |\omega(s)| \geq \epsilon. \quad (1)$$

The definition above is the standard PE definition as in e.g. Narendra and Annaswamy (1989), Ioannou and Sun (1995) and Khalil (1996), albeit in a slightly different form as presented in Lefeber (2000). In contrast, the modified definition below is necessary to study stability in a multi-robot case as shown later.

Definition 2.2 (cf. Alvarez Aguirre 2011): A continuous vector function $\Omega(t) = \text{col}(\omega_1(t), \dots, \omega_n(t))$ such that $\omega_i: \mathbb{R}^+ \rightarrow \mathbb{R}$, $i = 1, \dots, n$, is said to be PE if for all $i = 1, \dots, n$, $\omega_i(t)$ is bounded, Lipschitz, and constants $\delta_c > 0$ and $\epsilon > 0$ exist such that

$$\forall t \geq 0, \exists s : t - \delta_c \leq s \leq t \text{ such that } \prod_{i=1}^n |\omega_i(s)| \geq \epsilon. \quad (2)$$

In the following theorem we study stability of an equilibrium point of a linear time-varying system

$$\dot{x} = A(t)x \quad (3)$$

in which $x \in \mathbb{R}^n$ and $A(t)$ is continuous. For this system, we define the observability Gramian of the pair $(A(t), C)$, where C is such that $y = C(t)x$, as $W(t, t + \delta) = \int_t^{t+\delta} \Phi^T(\tau, t) C^T(\tau) C(\tau) \Phi(\tau, t) d\tau$, in which $\Phi(\tau, t)$ is the state transition matrix (Rugh 1993).

Theorem 2.3 (Khalil 1996): *Consider a linear time varying system (3). Let $V(t, x)$ be a continuously differentiable Lyapunov function candidate and furthermore, let $\dot{V}(t, x)$ denote its derivative along solutions of (3), i.e. $\dot{V}(t, x) = \frac{\partial V}{\partial t}(t, x(t)) + \frac{\partial V}{\partial x} A(t)x$. Assume that*

$$k_1 \|x\|^2 \leq V(t, x) \leq k_2 \|x\|^2, \quad (4)$$

$$\dot{V}(t, x) = -x^T C^T C x \leq 0, \quad (5)$$

$$W(t, t + \delta) \geq k_3 I, \quad (6)$$

where k_1, k_2 and k_3 are positive constants, I is the identity matrix of appropriate dimensions and $W(t, t + \delta)$ is the observability Gramian of the pair $(A(t), C)$. Then the origin of (3) is a globally exponentially stable equilibrium point.

Remark 1: Condition (6) is satisfied if the pair $(A(t), C)$ is completely uniformly observable, see (Khalil 1996).

Theorem 2.4 (Panteley and Loria 1998; Panteley, Lefeber, Loria, and Nijmeijer 1998; Aneke 2003): *Consider the cascaded system*

$$\begin{cases} \dot{x}_1 = f_1(t, x_1) + g(t, x_1, x_2)x_2, \\ \dot{x}_2 = f_2(t, x_2), \end{cases} \quad (7)$$

where $x_1 \in \mathbb{R}^p$, $x_2 \in \mathbb{R}^r$, $x = \text{col}(x_1, x_2)$, $f_1(t, x_1)$ is continuously differentiable in (t, x_1) and both $f_2(t, x_2)$ and $g(t, x_1, x_2)$ are continuous in t and locally Lipschitz in x . Assume that $f_1(t, 0) = 0$, $f_2(t, 0) = 0$ and

- (1) the equilibrium point $x_{e1} = 0$ of the subsystem $\dot{x}_1 = f_1(t, x_1)$ is globally exponentially stable,
- (2) the equilibrium point $x_{e2} = 0$ of the subsystem $\dot{x}_2 = f_2(t, x_2)$ is globally exponentially stable and
- (3) $g(t, x_1, x_2)$ satisfies $\|g(t, x_1, x_2)\| \leq k_1(\|x_2\|) + k_2(\|x_2\|)\|x_1\|$, in which $k_1, k_2: \mathbb{R}_0^+ \rightarrow \mathbb{R}_0^+$.

Then, the origin of the cascaded system (7) is globally \mathcal{K} -exponentially stable.

We refer to Sordalen and Egeland (1995) for a definition of global \mathcal{K} -exponential stability of an equilibrium point.

Definition 2.5 (Godsil and Royle 2001): A graph \mathcal{G} is a triple $\mathcal{G} = (\mathcal{V}, \mathcal{E}, \mathcal{A})$ where \mathcal{V} is an index set representing vertices, $\mathcal{E} \subset \mathcal{V} \times \mathcal{V}$ denotes edges such that an ordered pair $(i, j) \in \mathcal{E}$ iff there is an edge from vertex $i \in \mathcal{V}$ to vertex $j \in \mathcal{V}$, and \mathcal{A} is the adjacency matrix which has entries a_{ij} such that

$$a_{ij} = \begin{cases} 1 & \text{if } e_{ij} \in \mathcal{E}, \\ 0 & \text{otherwise.} \end{cases} \quad (8)$$

Hence, $\forall i, j \in \mathcal{V}$ we have $e_{ij} \in \mathcal{E}$ iff $a_{ij} = 1$.

Definition 2.6: $N_i \subset \mathcal{V}$ is the set of neighbours of vertex $i \in \mathcal{V}$ defined by

$$N_i = \{j \in \mathcal{V} \mid j \neq i \text{ and } a_{ij} \neq 0\}. \quad (9)$$

Definition 2.7 (Godsil and Royle 2001): A graph \mathcal{G} is called undirected if $(i, j) \in \mathcal{E}$ whenever $(j, i) \in \mathcal{E}$. It is said to be connected if any two vertices may be connected by a path regardless of the sequence of the vertices involved en route. Otherwise the graph is said to be disconnected.

3. Virtual structure formation control with mutual coupling

In this section we define the formation control problem under consideration and propose a formation control algorithm to solve this problem. In particular, in Section 3.1, the formation control problem is formulated and the kinematic model of a unicycle mobile robot is presented. Further, in Section 3.2, we give our main result that is a virtual structure formation controller, with mutual coupling between the robots. We also propose an extension of this algorithm in Section 3.3, designed to solve the formation control problem for dynamic models of the unicycle mobile robots.

3.1 Problem formulation

In this section we formulate the formation control problem that is studied in this article. We consider a formation of N identical nonholonomic unicycle mobile robots. The kinematics of the i th robot is described by the following differential equation:

$$\begin{aligned} \dot{x}_i &= v_i \cos(\phi_i), \\ \dot{y}_i &= v_i \sin(\phi_i), \\ \dot{\phi}_i &= \omega_i, \end{aligned} \quad (10)$$

with $i = 1, \dots, N$ and where the coordinates x_i and y_i describe the position of the centre of mass of the i th

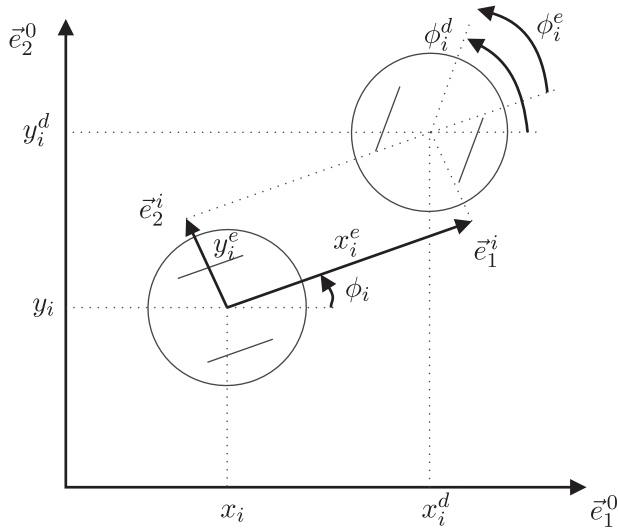


Figure 1. The unicycle coordinates, desired coordinates and error coordinates of the i th mobile robot.

mobile robot with respect to the fixed coordinate frame $\bar{e}^0 := [\bar{e}_1^0 \ \bar{e}_2^0]^T$ and the orientation ϕ_i is the angle between the heading of the i th robot and the x -axis of the fixed orthonormal coordinate frame \bar{e}^0 , see Figure 1. The forward velocity and rotational velocity are given by v_i and ω_i , respectively, and are, in this kinematic model, the control inputs of the i th mobile robot.

Following the virtual structure approach, an additional virtual robot with identical kinematics (10) as for all ordinary robots in the group is introduced. This virtual robot is placed in the so-called virtual centre of the formation. Note that the virtual centre does not need to be an actual geometric centroid of the formation but may be any point considered as central for a particular application. Based upon the position and orientation of the virtual centre, desired positions of robots in the formation are given with the aid of possibly time-varying bounded coordinates $p_i(t) = (p_{xi}(t), p_{yi}(t))^T$ given with respect to the local coordinate system \bar{e}^{vc} associated with the virtual robot that is in accordance to its orientation, see Figure 2. Assume that $\dot{p}_i(t)$ is bounded.

For the formation control problem to be solved, we require that the virtual structure follows a predefined trajectory $(x_{vc}^d(t), y_{vc}^d(t), \phi_{vc}^d(t))$, where $(x_{vc}^d(t), y_{vc}^d(t))$ denotes desired Cartesian positions and $\phi_{vc}^d(t)$ denotes a desired orientation of the virtual structure, and all robots in the formation maintain a given spatial pattern defined by the desired formation shape $p_i(t)$, $i = 1, \dots, N$. In terms of the behaviours of individual robots, this requirement is tantamount to

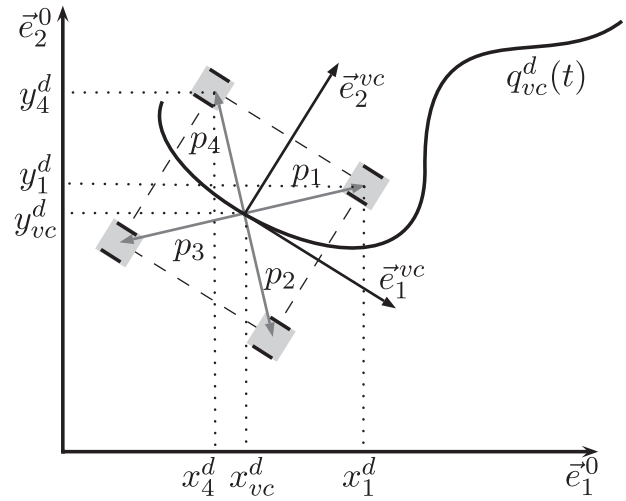


Figure 2. Desired positions of robots in the formation with respect to the virtual structure's position and a given formation shape.

the condition that the following set of equalities holds asymptotically

$$\begin{pmatrix} x_i(t) \\ y_i(t) \end{pmatrix} - \begin{pmatrix} x_i^d(t) \\ y_i^d(t) \end{pmatrix} = \begin{pmatrix} 0 \\ 0 \end{pmatrix}, \quad i = 1, \dots, N. \quad (11)$$

Here, $x_i^d(t)$ and $y_i^d(t)$ are calculated according to

$$\begin{aligned} x_i^d &= x_{vc}^d + p_{xi} \cos \phi_{vc}^d - p_{yi} \sin \phi_{vc}^d, \\ y_i^d &= y_{vc}^d + p_{xi} \sin \phi_{vc}^d + p_{yi} \cos \phi_{vc}^d, \end{aligned} \quad (12)$$

and represent the desired trajectories of individual robots in the fixed coordinate frame \bar{e}^0 that are determined specifically for a particular desired trajectory of the virtual structure and a particular desired formation shape. Moreover, the functions ϕ_{vc}^d and ϕ_i^d above follow from the nonholonomic, no-side-slip constraint $\dot{x} \sin \phi - \dot{y} \cos \phi = 0$ and (x_{vc}^d, y_{vc}^d) or (x_i^d, y_i^d) , respectively.

Remark 2: In the literature, control algorithms have been proposed that implement obstacle avoidance strategies on the level of desired trajectories, see e.g. Kostić, Adinandra, Caarls, and Nijmeijer (2010). Such algorithms for obstacle avoidance can also be integrated with the formation control strategy proposed in this article by feeding such adapted reference trajectories to the formation controller. Having said that, in this article we refrain from such a technical extension and concentrate on the formation control design as such.

Let v_{vc}^d and ω_{vc}^d be desired forward and angular velocities, respectively, associated with the desired trajectory $(x_{vc}^d(t), y_{vc}^d(t))$ of the virtual structure.

Assume that v_{vc}^d and ω_{vc}^d are bounded. By differentiating (12) and comparing the result with the desired kinematics of robot i in (10), one obtains desired velocities for each individual robot as follows:

$$\begin{aligned} v_i^d &= \sqrt{(\dot{x}_i^d)^2 + (\dot{y}_i^d)^2}, \\ \omega_i^d &= \frac{\ddot{y}_i^d \dot{x}_i^d - \ddot{x}_i^d \dot{y}_i^d}{(\dot{x}_i^d)^2 + (\dot{y}_i^d)^2}. \end{aligned} \quad (13)$$

The existence of these expressions is well-known in the robotics literature (Laumond 1998; Morin and Samson 2008) and is a consequence of the differential flatness of (9) (Fliess, Lévine, Martin, and Rouchon 1995).

Following Kanayama, Kimura, Miyazaki, and Noguchi (1990), the error variables of robot i are defined by

$$\begin{pmatrix} x_i^e \\ y_i^e \\ \phi_i^e \end{pmatrix} = \begin{bmatrix} \cos \phi_i & \sin \phi_i & 0 \\ -\sin \phi_i & \cos \phi_i & 0 \\ 0 & 0 & 1 \end{bmatrix} \begin{pmatrix} x_i^d - x_i \\ y_i^d - y_i \\ \phi_i^d - \phi_i \end{pmatrix}, \quad (14)$$

and correspond to the error coordinates in frame \tilde{e}^i , see Figure 1. Consequently, the error dynamics are given by

$$\begin{aligned} \dot{x}_i^e &= \omega_i y_i^e - v_i + v_i^d \cos \phi_i^e, \\ \dot{y}_i^e &= -\omega_i x_i^e + v_i^d \sin \phi_i^e, \\ \dot{\phi}_i^e &= \omega_i^d - \omega_i, \quad i = 1, \dots, N. \end{aligned} \quad (15)$$

Therefore, the formation control problem may be stated as follows: design controllers for v_i and ω_i that render the error dynamics (15) globally asymptotically stable.

3.2 Virtual structure control design

In this section, we design a virtual structure controller with mutual coupling between neighbouring individual robots that solves the formation control problem. The main goals of the virtual structure controller are twofold. Firstly, as mentioned earlier, the formation as a whole should follow a predefined trajectory, i.e. the virtual centre should follow a predefined trajectory and the i th unicycle robot, $i \in \{1, \dots, N\}$, should follow its desired individual trajectory dependent upon the desired trajectory of the virtual centre and the desired and possibly time-varying formation shape, determined by the coordinates (p_{xi}, p_{yi}) relative to the virtual centre. Secondly, if the individual robots suffer from perturbations, the controller should mediate between keeping formation and ensuring the tracking of the individual robots' desired trajectories, which is facilitated by introducing mutual coupling between the robots. To meet this double objective, we employ a

modified version of the control algorithm proposed originally for a single nonholonomic system by Panteley et al. (1998) and revisited afterwards by Jakubiak, Lefeber, Tchoń, and Nijmeijer (2002). The augmentation that is crucial for a formation control algorithm involves the inclusion of a mutual coupling between the robots. Therefore, for the i th robot we introduce additional mutual coupling terms $x_i^e - x_j^e$, $y_i^e - y_j^e$ and $\phi_i^e - \phi_j^e$ for each robot $j \in N_i$. Note that in Rodriguez-Angeles and Nijmeijer (2003, 2004) the concept of mutual coupling was employed in the synchronisation of industrial robots. However, in that work, the mutual coupling terms were introduced at the level of the desired trajectories. Here, we propose to introduce the coupling directly to each robot's control which results in the following controller:

$$\begin{aligned} v_i &= v_i^d + c_i^x x_i^e - c_i^y \omega_i^d y_i^e + \sum_{j \in N_i} \tilde{c}_{ij}^x (x_i^e - x_j^e) \\ &\quad - \sum_{j \in N_i} \tilde{c}_{ij}^y \omega_i^d (y_i^e - y_j^e), \\ \omega_i &= \omega_i^d + c_i^\phi \phi_i^e + \sum_{j \in N_i} \tilde{c}_{ij}^\phi (\phi_i^e - \phi_j^e), \quad i = 1, \dots, N, \end{aligned} \quad (16)$$

where c_i^x , c_i^y , c_i^ϕ for $i=1, \dots, N$ represent tracking control gains and \tilde{c}_{ij}^x , \tilde{c}_{ij}^y , \tilde{c}_{ij}^ϕ for $i=1, \dots, N$, $j \in N_i$ represent mutual coupling gains. Note that the original tracking algorithm for a single mobile robot proposed by Panteley et al. (1998) can be retrieved by setting all coupling gains to zero, i.e. $\tilde{c}_{ij}^x = 0$, $\tilde{c}_{ij}^y = 0$, $\tilde{c}_{ij}^\phi = 0$. In the case of formation control, these mutual coupling gains are crucial for robots in the formation to be aware of their neighbours' states. The importance of the mutual coupling terms can be particularly viewed if some of the robots in the formation are subject to a perturbation. Then the mutual coupling terms act in such a way that the remaining robots counteract the perturbation so that the desired formation shape may be preserved to some extent depending on the magnitude of the coupling gains, which is not the case when robots are unaware of their neighbours' behaviour. In other words, when the additional mutual coupling gains are combined with the tracking gains, the robots mediate between individual trajectory tracking and keeping a desired formation.

In the following theorem, we examine when the formation control problem as defined in this article is solved using the control law given in (16).

Theorem 3.1: Consider a group of N nonholonomic mobile robots (10), a desired trajectory of the virtual centre of the formation $(x_{vc}^d(t), y_{vc}^d(t))$, a desired

formation shape given by coordinates $p_i(t)$ that are bounded and such that $\dot{p}_i(t)$ are also bounded, and associated desired trajectories of robots in the formation (12) together with desired forward and angular velocities (13). Let the control law be defined in (16) in which $c_i^x, c_i^y, c_i^\phi, \tilde{c}_{ij}^x, \tilde{c}_{ij}^y, \tilde{c}_{ij}^\phi$ are positive parameters such that $\tilde{c}_{ij}^x = \tilde{c}_{ji}^x$ and $\tilde{c}_{ij}^y = \tilde{c}_{ji}^y$ and $\tilde{c}_{ij}^\phi \neq 0$ iff $j \in N_i$ for all $v \in \{x, y, \phi\}$. Assume that for $i=1, \dots, N$, $\omega_i^d(t)$ are such that $\bar{\Omega}^d(t) = \text{col}(\omega_1^d(t), \dots, \omega_N^d(t))$ satisfies the persistence of excitation condition in Definition 2.2, and $v_i^d(t)$ is non-zero and bounded from above, for all t . Then the origin is a globally K -exponentially stable equilibrium point of the closed-loop error dynamics (15)–(16) and hence the control law (16) solves the formation control problem.

Proof: Application of the control law (16) yields the

$$\mathbf{C}^x = \begin{bmatrix} c_1^x + \sum_{j \in N_1} \tilde{c}_{1j}^x & -\tilde{c}_{12}^x & \dots & -\tilde{c}_{1N}^x \\ \vdots & \ddots & \ddots & \vdots \\ -\tilde{c}_{N-11}^x & \ddots & c_{N-1}^x + \sum_{j \in N_{N-1}} \tilde{c}_{N-1j}^x & -\tilde{c}_{N-1N}^x \\ -\tilde{c}_{N1}^x & -\tilde{c}_{N2}^x & \dots & c_N^x + \sum_{j \in N_N} \tilde{c}_{Nj}^x \end{bmatrix}, \quad (18)$$

$$\mathbf{C}^y = \begin{bmatrix} c_1^y + \sum_{j \in N_1} \tilde{c}_{1j}^y & -\tilde{c}_{12}^y & \dots & -\tilde{c}_{1N}^y \\ \vdots & \ddots & \ddots & \vdots \\ -\tilde{c}_{N-11}^y & \ddots & c_{N-1}^y + \sum_{j \in N_{N-1}} \tilde{c}_{N-1j}^y & -\tilde{c}_{N-1N}^y \\ -\tilde{c}_{N1}^y & -\tilde{c}_{N2}^y & \dots & c_N^y + \sum_{j \in N_N} \tilde{c}_{Nj}^y \end{bmatrix}, \quad (19)$$

$$\mathbf{C}^\phi = \begin{bmatrix} c_1^\phi + \sum_{j \in N_1} \tilde{c}_{1j}^\phi & -\tilde{c}_{12}^\phi & \dots & -\tilde{c}_{1N}^\phi \\ \vdots & \ddots & \ddots & \vdots \\ -\tilde{c}_{N-11}^\phi & \ddots & c_{N-1}^\phi + \sum_{j \in N_{N-1}} \tilde{c}_{N-1j}^\phi & -\tilde{c}_{N-1N}^\phi \\ -\tilde{c}_{N1}^\phi & -\tilde{c}_{N2}^\phi & \dots & c_N^\phi + \sum_{j \in N_N} \tilde{c}_{Nj}^\phi \end{bmatrix}, \quad (20)$$

following closed-loop error dynamics of the overall formation

$$\underbrace{\begin{pmatrix} \dot{X}^e \\ \dot{Y}^e \end{pmatrix} = \begin{bmatrix} -\mathbf{C}^x & \Omega^d(\mathbf{C}^y + \mathbf{I}) \\ -\Omega^d & \mathbf{0} \end{bmatrix}}_{\dot{z}_1 = f_1(t, z_1)} \begin{pmatrix} X^e \\ Y^e \end{pmatrix} + \underbrace{\begin{bmatrix} \bar{\mathbf{Y}}^e \mathbf{C}^\phi + \mathbf{V}^d \Phi_{\cos} \\ -\bar{\mathbf{X}}^e \mathbf{C}^\phi + \mathbf{V}^d \Phi_{\sin} \end{bmatrix}}_{g(t, z_1, z_2)} \Phi^e, \quad \underbrace{\dot{\Phi}^e = -\mathbf{C}^\phi \Phi^e}_{\dot{z}_2 = f_2(z_2)}, \quad (17)$$

where $X^e = \text{col}(x_1^e, \dots, x_N^e)$, $Y^e = \text{col}(y_1^e, \dots, y_N^e)$, $\Phi^e = \text{col}(\phi_1^e, \dots, \phi_N^e)$, $\bar{\mathbf{X}}^e = \text{diag}(x_1^e, \dots, x_N^e)$, $\bar{\mathbf{Y}}^e = \text{diag}(y_1^e, \dots, y_N^e)$, \mathbf{I} is the identity matrix of appropriate dimensions, $\mathbf{0}$ is a matrix with all entries equal zero of appropriate dimensions, $\Omega^d = \text{diag}(\omega_1^d, \dots, \omega_N^d)$, $\mathbf{V}^d = \text{diag}(v_1^d, \dots, v_N^d)$,

$$\Phi_{\cos} = \text{diag}\left(\frac{\cos \phi_1^e - 1}{\phi_1^e}, \dots, \frac{\cos \phi_N^e - 1}{\phi_N^e}\right)$$

and

$$\Phi_{\sin} = \text{diag}\left(\frac{\sin \phi_1^e}{\phi_1^e}, \dots, \frac{\sin \phi_N^e}{\phi_N^e}\right).$$

Note that the functions $\frac{\sin \phi_i^e}{\phi_i^e}$ and $\frac{\cos \phi_i^e - 1}{\phi_i^e}$ are smooth if their definition is extended to $\phi_i^e = 0$ in the standard way. The remaining matrices \mathbf{C}^x , \mathbf{C}^y and \mathbf{C}^ϕ in (17) are given by:

where for $i \neq j$, we have $\mathbf{C}_{ij}^x \neq 0$, $\mathbf{C}_{ij}^y \neq 0$ and $\mathbf{C}_{ij}^\phi \neq 0$ iff $j \in N_i$. With the aid of the Geršgorin disc theorem (Horn and Johnson 1990), we can show that all eigenvalues of matrix \mathbf{C}^x lie in the region defined by

$$G(\mathbf{C}^x) = \bigcup_{i=1}^n \left\{ z \in \mathbb{C} \mid \left| z - \left(c_i^x + \sum_{j \in N_i} \tilde{c}_{ij}^x \right) \right| \leq \sum_{j \in N_i} \tilde{c}_{ij}^x \right\} \subset \mathbb{C}^+, \quad (21)$$

where \mathbb{C}^+ denotes the open right-half plane of the complex plane. Due the fact that \mathbf{C}^x is symmetric, it is apparent that \mathbf{C}^x is positive definite. Similarly, it may be shown that \mathbf{C}^y also is positive definite.

Clearly, the formation error dynamics (17) has the cascade form of (7). Thus, if the assumptions in Theorem 2.4 hold, the origin of (17) is globally \mathcal{K} -exponentially stable.

To show this, let us first consider the first stage of the cascade, i.e. $\dot{z}_1 = f_1(t, z_1)$:

$$\begin{cases} \dot{z}_{11} = -\mathbf{C}^x z_{11} + \mathbf{\Omega}^d (\mathbf{I} + \mathbf{C}^y) z_{12}, \\ \dot{z}_{12} = -\mathbf{\Omega}^d z_{11}, \end{cases} \quad (22)$$

in which $z_1 = \text{col}(z_{11}, z_{12}) := \text{col}(X^e, Y^e)$. Consider a Lyapunov function candidate for (22) of the form

$$V(z_{11}, z_{12}) = \frac{1}{2} (z_{11}^T z_{11} + z_{12}^T (\mathbf{I} + \mathbf{C}^y) z_{12}). \quad (23)$$

Then, the time derivative of (23) along trajectories of (22) yields

$$\begin{aligned} \dot{V}(z_{11}, z_{12}) &= -z_{11}^T \mathbf{C}^x z_{11} + z_{11}^T \mathbf{\Omega}^d (\mathbf{I} + \mathbf{C}^y) z_{12} \\ &\quad - z_{12}^T (\mathbf{I} + \mathbf{C}^y) \mathbf{\Omega}^d z_{11} = -z_{11}^T \mathbf{C}^x z_{11} \leq 0, \end{aligned} \quad (24)$$

where the second equality holds because \mathbf{C}^y is symmetric and the inequality follows from the fact that \mathbf{C}^x is positive definite. Additionally, from Theorem 2.3 we know that $z_1 = 0$ is a globally exponentially stable equilibrium point of (22) if, besides (24), the observability Gramian of the pair $(A(t), C)$ satisfies (6) where

$$A(t) = \begin{bmatrix} -\mathbf{C}^x & \mathbf{\Omega}^d (\mathbf{C}^y + \mathbf{I}) \\ -\mathbf{\Omega}^d & \mathbf{0} \end{bmatrix}, \quad C = \begin{bmatrix} \sqrt{\frac{1}{2} \mathbf{C}^x} & \mathbf{0} \\ \sqrt{\frac{1}{2} \mathbf{C}^x} & \mathbf{0} \end{bmatrix}. \quad (25)$$

Following the developments in Khalil (1996) and Alvarez Aguirre (2011) it can indeed be shown that given the fact that $\tilde{\Omega}^d(t)$ is PE according to Definition 2.2, the pair $(A(t), C)$ is completely uniformly observable and hence Condition (6) is satisfied. Thus, Theorem 2.3 can be used to show that $z_1 = 0$ is a globally exponentially stable equilibrium of (22) which proves the validity of Assumption 1 in Theorem 2.4.

The second assumption from Theorem 2.4 can be proven to be true immediately since $\dot{z}_2 = f_2(z_2)$ represents the following linear time-invariant system:

$$\dot{\Phi}^e = -\mathbf{C}^\phi \Phi^e. \quad (26)$$

Once again using the Geršgorin disc theorem (Horn and Johnson 1990), it may be shown that all eigenvalues of \mathbf{C}^ϕ lie in \mathbb{C}^+ . Hence, $\Phi^e = 0$ is a globally exponentially stable equilibrium point of (26). This proves Assumption 2 in Theorem 2.4.

Next, let us show that $g(t, z_1, z_2)$ from (17) satisfies Assumption 3 from Theorem 2.4. After some manipulations, we obtain

$$\|g(t, z_1, z_2)\|_F \leq 2Nv^* + \|\mathbf{C}^\phi\| \|z_1\|, \quad (27)$$

where

$$\begin{aligned} v_i^* &= \sup\{|v_i^d(t)| \mid t \geq 0\}, \\ v^* &= \max\{v_i^* \mid i = 1, \dots, N\}, \end{aligned} \quad (28)$$

and $\|\cdot\|_F$ denotes the Frobenius norm, see Khalil (1996). Note that boundedness of v_i^d is implied by boundedness of v_{vc}^d , ω_{vc}^d , p_i and \dot{p}_i as assumed. Hence, Assumption 3 in Theorem 2.4 is satisfied with $k_1(\cdot) = 2Nv^*$ and $k_2(\cdot) = \|\mathbf{C}^\phi\|$. Therefore it follows from Theorem 2.4 that the origin $(z_1, z_2) = (0, 0)$ of the cascade system (17) is globally \mathcal{K} -exponentially stable. Therefore, the control law (16) solves the formation control problem studied in this article.

This completes the proof. \square

Remark 3: Theorem 3.1 only poses rather weak constraints on the control parameters. Therefore, there is a considerable freedom to design the control parameters in a way which is desirable for a specific application. In particular, to focus on tracking of individual robots' trajectories, the tracking gains c_i^x, c_i^y, c_i^ϕ should dominate the mutual coupling gains $\tilde{c}_{ij}^x, \tilde{c}_{ij}^y, \tilde{c}_{ij}^\phi$. On the other hand, when keeping formation is the major objective, the mutual coupling gains $\tilde{c}_{ij}^x, \tilde{c}_{ij}^y$ and \tilde{c}_{ij}^ϕ ought to dominate the tracking gains c_i^x, c_i^y, c_i^ϕ .

Remark 4: The condition $c_i^y > 0$ may be weakened to $c_i^y > -1$. This is because we only require matrix $(\mathbf{I} + \mathbf{C}^y)$ in (23) to be a positive-definite matrix, as opposed to matrix \mathbf{C}^y being positive definite. However, it was noted in van den Broek, van de Wouw, and Nijmeijer (2009) that the choice of a negative control parameter c_i^y may cause some undesirable transient behaviour of robots in the formation.

3.3 Dynamic control law

In this section we consider a distributed dynamic formation control algorithm based on a simple dynamic model of a mobile robot (Jiang and Nijmeijer 1997; Panteley et al. 1998):

$$\begin{aligned} \dot{x}_i &= v_i \cos \phi_i, \\ \dot{y}_i &= v_i \sin \phi_i, \\ \dot{\phi}_i &= \omega_i, \\ \dot{v}_i &= \frac{F_i}{m_i}, \\ \dot{\omega}_i &= \frac{\tau_i}{J_i}, \end{aligned} \quad (29)$$

in which m_i denotes the mass of the i th robot, J_i is its moment of inertia around the vertical axis passing through its centre of mass and the control inputs F_i and τ_i denote force and torque respectively.

The dynamic formation control algorithm is an extension of the kinematic control law presented in the previous section and is motivated by the developments in Panteley et al. (1998). Based on the control law defined in Theorem 3.1, we define nominal forward and angular velocities as

$$\begin{aligned}\bar{v}_i &= v_i^d + c_i^x x_i^e - c_i^y \omega_i^d y_i^e + \sum_{j \in N_i} \tilde{c}_{ij}^x (x_i^e - x_j^e) \\ &\quad - \sum_{j \in N_i} \tilde{c}_{ij}^y \omega_i^d (y_i^e - y_j^e), \\ \bar{\omega}_i &= \omega_i^d + c_i^\phi \phi_i^e + \sum_{j \in N_i} \tilde{c}_{ij}^\phi (\phi_i^e - \phi_j^e).\end{aligned}\quad (30)$$

Also, we define additional velocity error variables by

$$\begin{aligned}v_i^e &= v_i - \bar{v}_i \\ \omega_i^e &= \omega_i - \bar{\omega}_i.\end{aligned}\quad (31)$$

Differentiating (31), we obtain time derivatives of the new error variables defined along solutions of (29) for each robot $i = 1, \dots, N$ in the formation:

$$\begin{aligned}\dot{v}_i^e &= \frac{F_i}{m_i} - \dot{\bar{v}}_i, \\ \dot{\omega}_i^e &= \frac{\tau_i}{J_i} - \dot{\bar{\omega}}_i.\end{aligned}\quad (32)$$

Combining (15) and (32) yields the following error dynamics:

$$\begin{aligned}\dot{x}_i^e &= \bar{\omega}_i y_i^e - \bar{v}_i + v_i^d \cos \phi_i^e + \omega_i^e y_i^e - v_i^e, \\ \dot{y}_i^e &= -\bar{\omega}_i x_i^e + v_i^d \sin \phi_i^e - \omega_i^e x_i^e, \\ \dot{\phi}_i^e &= \omega_i^d - \bar{\omega}_i - \omega_i^e, \\ \dot{v}_i^e &= \frac{F_i}{m_i} - \dot{\bar{v}}_i, \\ \dot{\omega}_i^e &= \frac{\tau_i}{J_i} - \dot{\bar{\omega}}_i,\end{aligned}\quad (33)$$

for which we should design control laws for F_i and τ_i , such that it exhibits a globally asymptotically stable equilibrium point at the origin. Using the expressions of \bar{v}_i and $\bar{\omega}_i$ in (30), we obtain the following error dynamics for the overall formation

$$\begin{aligned}\begin{pmatrix} \dot{X}^e \\ \dot{Y}^e \\ \dot{V}^e \end{pmatrix} &= \begin{bmatrix} -C^x & \Omega^d(C^y + I) & -I \\ -\Omega^d & 0 & 0 \\ 0 & 0 & 0 \end{bmatrix} \begin{pmatrix} X^e \\ Y^e \\ V^e \end{pmatrix} \\ &\quad + \begin{pmatrix} 0 \\ 0 \\ I \end{pmatrix} (M^{-1}F - \dot{\bar{V}})\end{aligned}$$

$$\begin{aligned}&+ \begin{bmatrix} \bar{Y}^e C^\phi + V^d \Phi_{\cos} & \bar{Y}^e \\ -\bar{X}^e C^\phi + V^d \Phi_{\sin} & -\bar{X}^e \\ 0 & 0 \end{bmatrix} \begin{pmatrix} \Phi^e \\ \Omega^e \end{pmatrix}, \\ \begin{pmatrix} \dot{\Phi}^e \\ \dot{\Omega}^e \end{pmatrix} &= \begin{bmatrix} -C^\phi & -I \\ 0 & 0 \end{bmatrix} \begin{pmatrix} \Phi^e \\ \Omega^e \end{pmatrix} + \begin{pmatrix} 0 \\ I \end{pmatrix} (J^{-1}T - \dot{\bar{\Omega}}),\end{aligned}\quad (34)$$

where $V^e = \text{col}(v_1^e, \dots, v_N^e)$, $\Omega^e = \text{col}(\omega_1^e, \dots, \omega_N^e)$, $M = \text{diag}(m_1, \dots, m_N)$, $J = \text{diag}(J_1, \dots, J_N)$, $F = \text{col}(F_1, \dots, F_N)$, $T = \text{col}(\tau_1, \dots, \tau_N)$, $\bar{V} = \text{col}(\bar{v}_1, \dots, \bar{v}_N)$ and $\bar{\Omega} = \text{col}(\bar{\omega}_1, \dots, \bar{\omega}_N)$. Moreover, the constant matrices C^x , C^y and C^ϕ are defined in (18)–(20). The control design, as motivated by Panteley et al. (1998), now relies on defining the control inputs F and T for the whole formation in such a way that the resultant closed-loop error dynamics have a cascade structure as in (7) and are globally \mathcal{K} -exponentially stable.

To this end, we propose the following control input:

$$\begin{aligned}F &= M(\dot{\bar{V}} + C^{vx} X^e - C^{vv} V^e), \\ T &= J(\dot{\bar{\Omega}} - C^\omega \Omega^e),\end{aligned}\quad (35)$$

where $C^{vx} = \text{diag}(c_1^{vx}, \dots, c_n^{vx})$, $C^{vv} = \text{diag}(c_1^{vv}, \dots, c_n^{vv})$ and $C^\omega = \text{diag}(c_1^\omega, \dots, c_n^\omega)$ are positive-definite matrices or, equivalently,

$$\begin{aligned}F_i &= m_i(\dot{\bar{v}}_i + c_i^{vx} x_i^e - c_i^{vv} v_i^e), \\ \tau_i &= J_i(\dot{\bar{\omega}}_i - c_i^\omega \omega_i^e).\end{aligned}\quad (36)$$

It will be shown in the following theorem that indeed application of the control law (35) to the formation of mobile robots with the open-loop error dynamics (34) globally exponentially stabilises the formation error dynamics (34).

Theorem 3.2: Consider N unicycle mobile robots satisfying (29), a desired trajectory of the virtual centre of the formation (x_{vc}^d, y_{vc}^d) and a desired formation shape $p_i(t)$, $i = 1, \dots, N$, such that both $p_i(t)$ and $\dot{p}_i(t)$ are bounded. Consider the control law defined in (36), where c_i^{vx} , c_i^{vv} , c_i^ω are positive parameters, both \bar{v}_i and $\bar{\omega}_i$ are defined in (30) and additional kinematic control parameters in (30) satisfy the conditions given in Theorem 3.1. Assume that for all $i = 1, \dots, N$, $\omega_i^d(t)$ in (13) is such that $\tilde{\Omega}^d(t) = \text{col}(\omega_1^d(t), \dots, \omega_N^d(t))$ satisfies the persistence of excitation condition in Definition 2.2, and $v_i^d(t)$ in (13) is non-zero and bounded. Then, the origin of the closed-loop error dynamics (29, 36) is globally \mathcal{K} -exponentially stable and hence, the formation control problem is solved.

Proof: The error dynamics of the whole formation controlled by (35) are

$$\begin{aligned} \underbrace{\begin{pmatrix} \dot{X}^e \\ \dot{Y}^e \\ \dot{V}^e \end{pmatrix}}_{\dot{z}_1=f_1(t, z_1)} &= \underbrace{\begin{bmatrix} -\mathbf{C}^x & \mathbf{\Omega}^d(\mathbf{C}^y + \mathbf{I}) & -\mathbf{I} \\ -\mathbf{\Omega}^d & \mathbf{0} & \mathbf{0} \\ \mathbf{C}^{vx} & \mathbf{0} & -\mathbf{C}^{vv} \end{bmatrix}}_{\mathbf{A}} \underbrace{\begin{pmatrix} X^e \\ Y^e \\ V^e \end{pmatrix}}_{\mathbf{z}_1} \\ &+ \underbrace{\begin{bmatrix} \bar{\mathbf{Y}}^e \mathbf{C}^\phi + \mathbf{V}^d \mathbf{\Phi}_{\cos} & \bar{\mathbf{Y}}^e \\ -\bar{\mathbf{X}}^e \mathbf{C}^\phi + \mathbf{V}^d \mathbf{\Phi}_{\sin} & -\bar{\mathbf{X}}^e \\ \mathbf{0} & \mathbf{0} \end{bmatrix}}_{\mathbf{g}(z_1, z_2)} \underbrace{\begin{pmatrix} \Phi^e \\ \Omega^e \end{pmatrix}}_{\mathbf{z}_2} \\ \underbrace{\begin{pmatrix} \dot{\Phi}^e \\ \dot{\Omega}^e \end{pmatrix}}_{\dot{z}_2=f_2(z_2)} &= -\underbrace{\begin{bmatrix} \mathbf{C}^\phi & \mathbf{I} \\ \mathbf{0} & \mathbf{C}^\omega \end{bmatrix}}_{\mathbf{H}} \underbrace{\begin{pmatrix} \Phi^e \\ \Omega^e \end{pmatrix}}_{\mathbf{z}_2}, \end{aligned} \quad (37)$$

which clearly has the cascade structure as in (7). Thus, if the three assumptions of Theorem 2.4 are satisfied, then the origin of (37) is a globally \mathcal{K} -exponentially stable equilibrium. To prove that this is indeed the case, consider the first stage of the cascade system, $\dot{z}_1=f_1(t, z_1)$, which is a linear time-varying system of the form

$$\begin{cases} \dot{z}_{11} = -\mathbf{C}^x z_{11} + \mathbf{\Omega}^d (\mathbf{I} + \mathbf{C}^y) z_{12} - z_{13}, \\ \dot{z}_{12} = -\mathbf{\Omega}^d z_{11}, \\ \dot{z}_{13} = \mathbf{C}^{vx} z_{11} - \mathbf{C}^{vv} z_{13}, \end{cases} \quad (38)$$

where $z_1 = \text{col}(z_{11}, z_{12}, z_{13}) := \text{col}(X^e, Y^e, V^e)$. Let us define a positive-definite Lyapunov function candidate for this system by

$$V(z_1) = \frac{1}{2} (z_{11}^T z_{11} + z_{12}^T (\mathbf{C}^y + \mathbf{I}) z_{12} + z_{13}^T (\mathbf{C}^{vx})^{-1} z_{13}). \quad (39)$$

By differentiating (39) with respect to time along trajectories of (38), one arrives at

$$\begin{aligned} \dot{V}(z_{11}, z_{12}, z_{13}) &= -z_{11}^T \mathbf{C}^x z_{11} + z_{11}^T \mathbf{\Omega}^d (\mathbf{I} + \mathbf{C}^y) z_{12} - z_{11}^T z_{13} \\ &\quad - z_{11}^T \mathbf{\Omega}^d (\mathbf{I} + \mathbf{C}^y) z_{12} + z_{13}^T (\mathbf{C}^{vx})^{-1} \mathbf{C}^{vx} z_{11} \\ &\quad - z_{13}^T (\mathbf{C}^{vx})^{-1} \mathbf{C}^{vv} z_{13} \\ &= -z_{11}^T \mathbf{C}^x z_{11} - z_{13}^T (\mathbf{C}^{vx})^{-1} \mathbf{C}^{vv} z_{13} \leq 0. \end{aligned} \quad (40)$$

Consequently, using similar arguments as in the proof of Theorem 3.1, we can prove by Theorem 2.3 that the origin $z_1=0$ is a globally exponentially stable equilibrium. Thus, Assumption 1 of Theorem 2.4 holds.

As for Assumption 2 in Theorem 2.4, let us rewrite subsystem $\dot{z}_2=f_2(z_2)$ as

$$\dot{z}_2 = -\begin{bmatrix} \mathbf{C}^\phi & \mathbf{I} \\ \mathbf{0} & \mathbf{C}^\omega \end{bmatrix} z_2 =: -\mathbf{H} z_2, \quad (41)$$

which is a time-invariant linear system. Because \mathbf{H} is an upper block triangular matrix, the set of its eigenvalues is created by merging the sets of eigenvalues of \mathbf{C}^ϕ and \mathbf{C}^ω . As shown before, all eigenvalues of \mathbf{C}^ϕ have positive real parts. Moreover, \mathbf{C}^ω is a positive-definite diagonal matrix. Therefore, all eigenvalues of both \mathbf{C}^ϕ and \mathbf{C}^ω lie in the open right half of the complex plane and so do all eigenvalues of \mathbf{H} . Thus, (41) is globally exponentially stable which proves Assumption 2 of Theorem 2.4.

As for Assumption 3 in Theorem 2.4, it may be easily shown that

$$\|g(t, z_1, z_2)\|_F \leq 2Nv^* + \|\mathbf{C}^\phi + \mathbf{I}\| \|z_1\|, \quad (42)$$

in which v^* is defined in (28) and $\|\cdot\|_F$ denotes the Frobenius norm (Khalil 1996). Hence Assumption 3 in Theorem 2.4 is satisfied with $k_1(\cdot)=2Nv^*$ and $k_2(\cdot)=\|\mathbf{C}^\phi + \mathbf{I}\|$. Therefore, by Theorem 2.4, the origin of the cascaded system (37) is globally \mathcal{K} -exponentially stable. Hence, the dynamic formation control problem studied in this article is solved.

This completes the proof. \square

Remark 5: As in the kinematic control algorithm, see Remark 3, also in the dynamic formation control algorithm, there is a trade-off between two control objectives: tracking of individual robot trajectories and keeping formation. Regarding pure trajectory tracking, this objective may be influenced by setting appropriate kinematic tracking gains c_i^x, c_i^y, c_i^ϕ or dynamic tracking parameters $c_i^{vx}, c_i^{vy}, c_i^\omega$. In turn, the formation geometry maintenance can be affected by mutual coupling terms $\tilde{c}_{ij}^x, \tilde{c}_{ij}^y$ and \tilde{c}_{ij}^ϕ .

4. Simulation study

In this section, we illustrate the behaviour of robots in a formation when the two control algorithms proposed in Section 3 are applied. We consider the case of three robots with two different communication structures: a connected one, as illustrated in Figure 3(a), and a disconnected one, as illustrated in Figure 3(b).

For both connected and disconnected communication networks, we allow for perturbations to occur. In particular, we consider the perturbation of Robot 1 due to a displacement of this robot at time $t=200$ from its current position along $(\delta x, \delta y)=(15, -26)$ in the $\bar{\mathcal{E}}^0$ frame. This perturbation, although unrealistic in

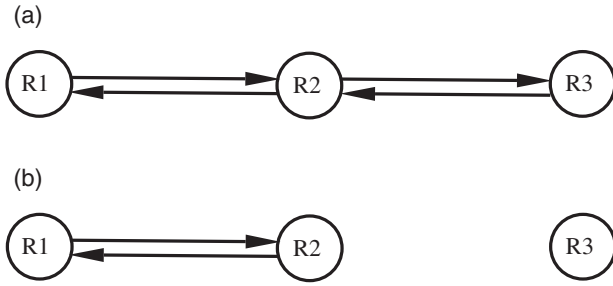


Figure 3. Communication graph structures used in simulations: (a) connected graph and (b) disconnected graph.

practice, serves well to present behaviour of robots in the formation in the presence of perturbations.

In all simulations in this section we consider a formation geometry maintenance index defined as follows. Let $r_i(t) = \text{col}(x_i(t), y_i(t))$ denote a robot's actual position with respect to the inertial coordinate frame \bar{e}^0 and $p_i(t)$ a robot's desired position in the formation relative to the virtual centre. Then the formation geometry maintenance index is defined according to

$$I(t) = \sum_{i=1}^3 \sum_{j=1, j \neq i}^3 (\|r_i(t) - r_j(t)\| - \|p_i(t) - p_j(t)\|)^2, \quad (43)$$

which shows discrepancy between actual formation shape and the desired one. In particular, it measures the difference between actual and desired distances between all pairs of robots in the formation. Note that $I(t) = 0$ occurs if and only if the formation shape is maintained, modulo a rotation or a reflection (a mirror image). We still consider a formation shape to be maintained despite a possible rotation or a reflection because we are purely interested here in verifying the geometric shape of the formation.

We choose the desired trajectory of the formation's virtual structure as

$$\begin{aligned} \dot{x}_{vc}^d &= 5 \cos \phi_{vc}^d, \\ \dot{y}_{vc}^d &= 5 \sin \phi_{vc}^d, \\ \dot{\phi}_{vc}^d &= 0.2 \sin t, \end{aligned} \quad (44)$$

in which $x_{vc}^d(0) = 0$, $y_{vc}^d(0) = 0$ and $\phi_{vc}^d(0) = 0$. Moreover, initial conditions of robots in the formation are given by $(x_1(0), y_1(0), \phi_1(0)) = (-23.56, 4.01, -\frac{\pi}{3})$, $(x_2(0), y_2(0), \phi_2(0)) = (5, 1.23, -\pi)$ and $(x_3(0), y_3(0), \phi_3(0)) = (12, 15.55, \frac{\pi}{2})$. Furthermore, the desired formation shape is defined via $p_1 = (-10, -\frac{10\sqrt{3}}{3})^T$, $p_2 = (10, -\frac{10\sqrt{3}}{3})^T$ and $p_3 = (0, \frac{20\sqrt{3}}{3})^T$ and forms an equilateral triangle as illustrated in Figure 4 in which

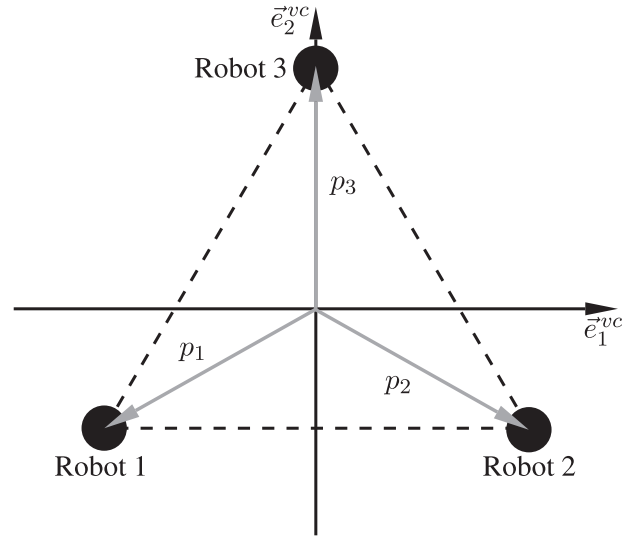


Figure 4. Desired formation geometry used in the simulations and experiments.

Table 1. List of control parameters used in simulations in Section 4.1. Note that in the case of a disconnected communication graph, coupling gains \tilde{c}_{23}^v and \tilde{c}_{32}^v for $v \in \{x, y, \phi\}$ are set to 0.

Robot 1	$c_1^x = 6$ $\tilde{c}_{12}^x = 19$ $\tilde{c}_{13}^x = 0$	$c_1^y = 4$ $\tilde{c}_{12}^y = 15$ $\tilde{c}_{13}^y = 0$	$c_1^\phi = 0.1$ $\tilde{c}_{12}^\phi = 3$ $\tilde{c}_{13}^\phi = 0$
Robot 2	$c_2^x = 6$ $\tilde{c}_{21}^x = 19$ $\tilde{c}_{23}^x = 27$	$c_2^y = 1.5$ $\tilde{c}_{21}^y = 15$ $\tilde{c}_{23}^y = 15$	$c_2^\phi = 0.3$ $\tilde{c}_{21}^\phi = 3$ $\tilde{c}_{23}^\phi = 3$
Robot 3	$c_3^x = 2$ $\tilde{c}_{31}^x = 0$ $\tilde{c}_{32}^x = 27$	$c_3^y = 3$ $\tilde{c}_{31}^y = 0$ $\tilde{c}_{32}^y = 15$	$c_3^\phi = 0.5$ $\tilde{c}_{31}^\phi = 0$ $\tilde{c}_{32}^\phi = 3$

the length of the sides equals 20. All simulations in this section are performed for the period of time $t \in [0, 300]$.

4.1 Kinematic formation control algorithm

In this section we present simulation results regarding the kinematic formation control law given in Section 3.2. Besides the simulation settings introduced in the introduction of this section, the additional control parameters are summarised in Table 1.

With such a choice of simulation settings, all conditions in Theorem 3.1 are now met and hence global exponential stability of the formation error dynamics is guaranteed. The simulations presented next will, firstly, illustrate that the robots (asymptotically) form the desired formation. Secondly, they will illustrate the benefit of mutual coupling between the

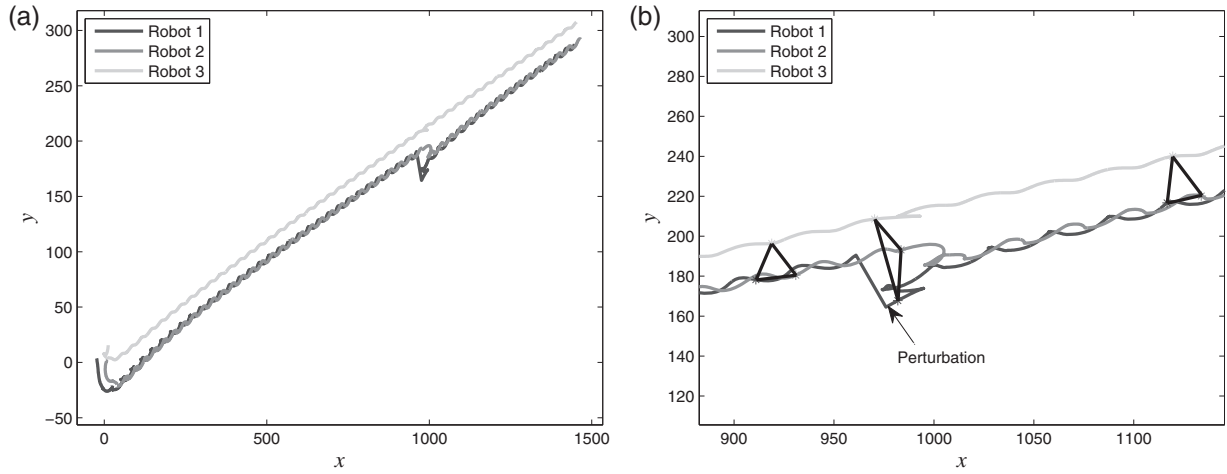


Figure 5. Robot paths on the plane in the case of a connected communication graph and the kinematic control algorithm (16): (a) whole paths and (b) zoomed-in part of the paths during the perturbation.

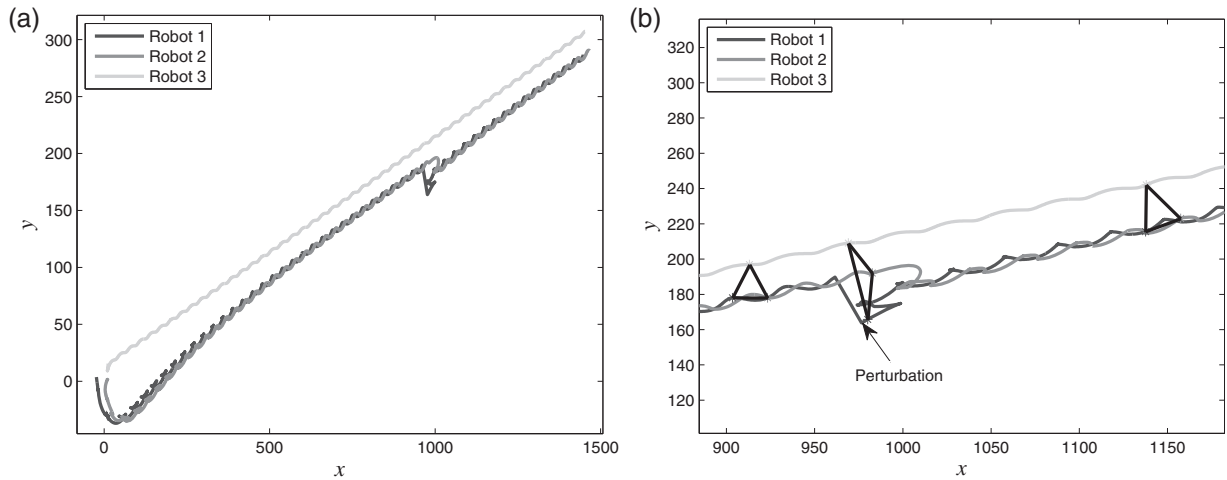


Figure 6. Robot paths on the plane in the case of a disconnected communication graph and the kinematic control algorithm (16): (a) whole paths and (b) zoomed-in part of the paths during the perturbation.

robots in terms of the robustness of the formation keeping properties in the face of perturbations and the convergence speed with which the robots form the desired formation. The simulation results are shown in Figures 5–7. In Figure 5, we depict robots' paths in the case of the connected communication graph of the formation in Figure 3(a). For the sake of convenience, in Figure 5(b), we zoom in on the part of the plot when the perturbation occurs to show in more detail the robots' paths. Evidently, robots in the formation converge to the desired formation geometry which is the equilateral triangle. Then, when Robot 1 is perturbed, the unperturbed robots abandon temporarily their desired trajectories in favour of keeping formation geometry. This is due to the particular

choice of mutual coupling terms \tilde{c}_{ij}^x , \tilde{c}_{ij}^y , \tilde{c}_{ij}^ϕ which dominate chosen tracking control gains c_i^x , c_i^y and c_i^ϕ .

The results are different when the communication graph is disconnected, see Figure 6. Although the formation shape seems to be restored, when the perturbation takes place, only Robot 1 and Robot 2 try to counteract its effect and keep the formation shape while Robot 3 is unaware of the perturbation and thus it does not divert from its desired trajectory in order for the formation shape to be maintained. This affects the value of the formation geometry maintenance index, see Figure 7. After the perturbation, the formation geometry maintenance index is larger in the case of the disconnected communication graph than in the case of the connected communication graph.

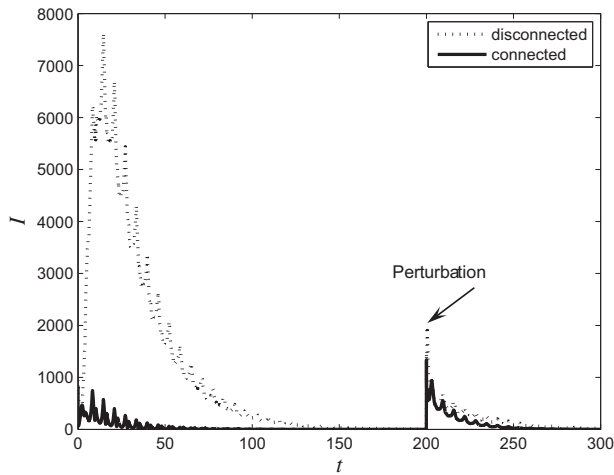


Figure 7. Comparison between formation geometry maintenance index I using the kinematic control algorithm for a connected and a disconnected communication graph.

Something similar may also be observed at the beginning of the simulations. As a result of nonzero initial conditions, the formation geometry maintenance index is also non-zero and converges to zero faster when the connectivity condition of the communication graph holds.

We summarise our findings in the following remark.

Remark 6: Formation behaviour under the formation control law in (16) can be improved if the communication graph \mathcal{G} of the formation is connected. This requirement stems from the fact that each robot needs to be able to exchange information with the rest of the group so that every member of the formation is aware of the actual performance of the whole group. Only if the communication graph is connected, we can be sure that the actual performance is known to each robot through their neighbours. This guarantees that the two objectives of trajectory tracking and formation keeping are achieved individually. On the other hand, when the communication graph of the formation is disconnected, one obtains pure trajectory tracking by some of the robots. By implication this also solves the formation control problem, but as illustrated by the simulation results, a better performance in terms of the robustness of the formation with respect to perturbations may be obtained when the communication graph is indeed connected.

4.2 Dynamic formation control algorithm

In this section we present the simulation results for the dynamic formation control law given in

Table 2. List of control parameters used in simulations in Section 4.2.

Robot 1	$c_1^{vv} = 15$	$c_1^{vx} = 15$	$c_2^{\omega} = 15$
Robot 2	$c_2^{vv} = 15$	$c_2^{vx} = 15$	$c_2^{\omega} = 15$
Robot 3	$c_3^{vv} = 9$	$c_3^{vx} = 9$	$c_3^{\omega} = 15$

Section 3.3. We provide all control parameters used in the simulations appearing in this section in Tables 1 and 2.

In Figure 8, robot paths in the case of a connected communication graph are shown. It can be concluded that initially all robots converge to their desired position in the formation and form the shape of the equilateral triangle. This situation changes entirely when a perturbation is applied to Robot 1. Interestingly, even though only Robot 1 is perturbed, both remaining robots also adjust their positions to keep the desired geometry. This comes about on account of the mutual coupling terms that cause the robots to again face a trade-off between trajectory tracking and formation shape preservation, as in the case of the kinematic control law in the previous subsection. It may be seen in Figure 8(b) that when Robot 1 is perturbed, both Robot 2 and Robot 3 react to this perturbation so that the perturbation is counteracted and the formation shape remains close to the desired formation geometry in the transient after the perturbation. On the other hand, in the case of a disconnected communication graph Robot 3 does not react when the perturbation occurs, as illustrated in Figure 9(b) which presents the part of paths of the robots during the perturbations.

As in the previous set of simulations, we can even more clearly observe the advantage of having a connected communication graph by presenting the formation geometry maintenance index, see Figure 10. In particular, we can observe two positive aspects of such a communication structure. First of all, the index has a larger magnitude in the case of the communication graph being disconnected both at the beginning of the simulations and when the perturbation occurs. Moreover, it approaches zero at a faster rate when the communication graph is connected.

5. Experiments

In this section, experimental results are presented to validate practical applicability of the controller design proposed in Section 3. In Section 5.1, the experimental setup is presented and experimental results are discussed in Section 5.2.

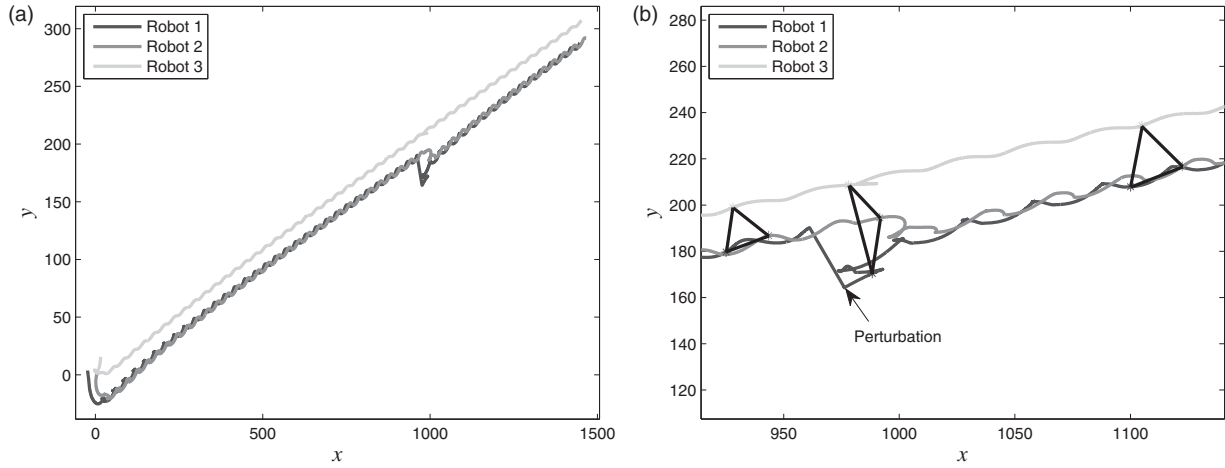


Figure 8. Robot paths on the plane in the case of a connected communication graph and the dynamic control algorithm (36): (a) whole paths and (b) zoomed-in part of the paths during the perturbation.

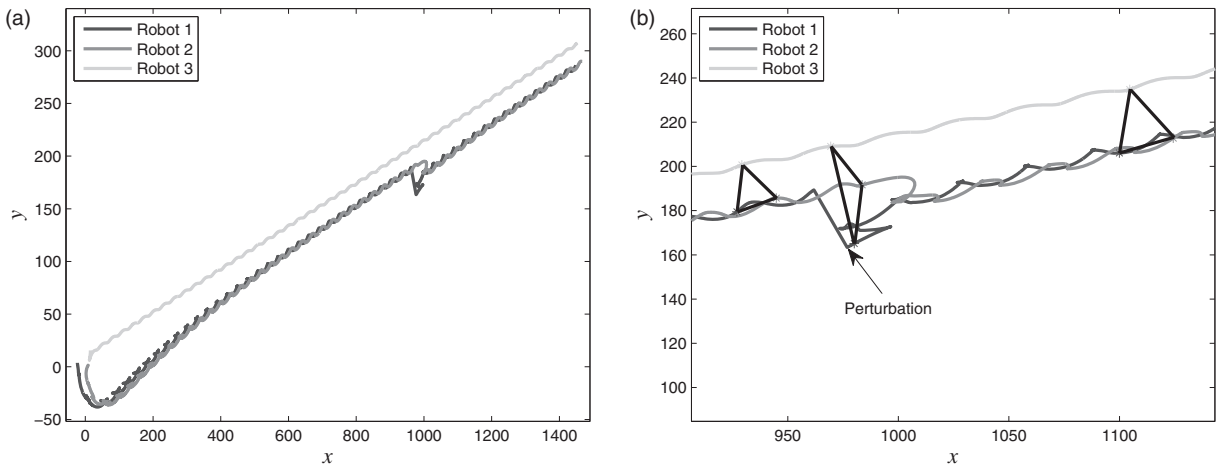


Figure 9. Robot paths on the plane in the case of a disconnected communication graph and the dynamic control algorithm (36): (a) whole paths and (b) zoomed-in part of the paths during the perturbation.

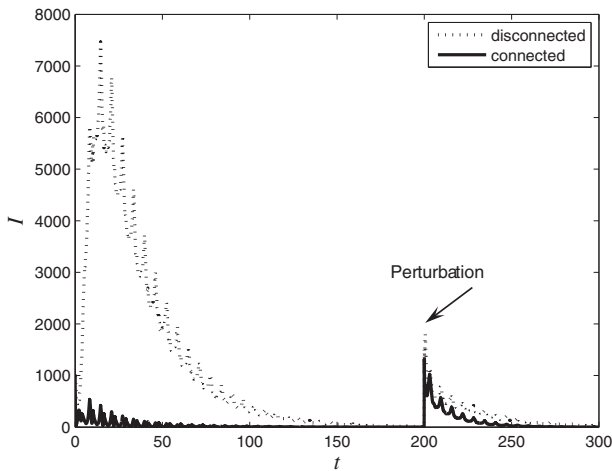
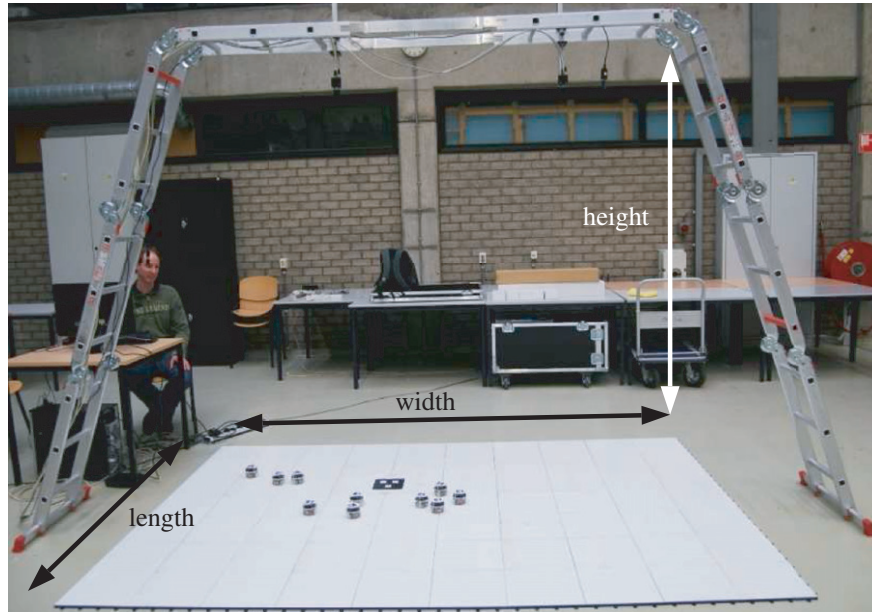


Figure 10. Comparison between formation geometry maintenance index I using the dynamic control algorithm for a connected and a disconnected communication graph.

5.1 Experimental setup

The experimental setup is shown in Figure 11. The experiments are performed with three E-Puck mobile robots (Mondada and Bonani 2007). The E-Puck robot has two driven wheels, which are individually actuated by means of stepper motors. Moreover, we use a camera as a localisation device for getting the position and orientation of all robots, and a PC. The PC generates robot trajectories, processes camera images to get the actual pose of the robots, and runs the control laws for all the robots. The control velocities are sent from the PC to the robots via a Bluetooth protocol. This way of implementation is chosen due to the limiting processing power of the onboard robot processors and due to the limited bandwidth of the Bluetooth communication.



The arena: length= 2.2 (m), width= 3.2 (m), height= 2.3 (m).

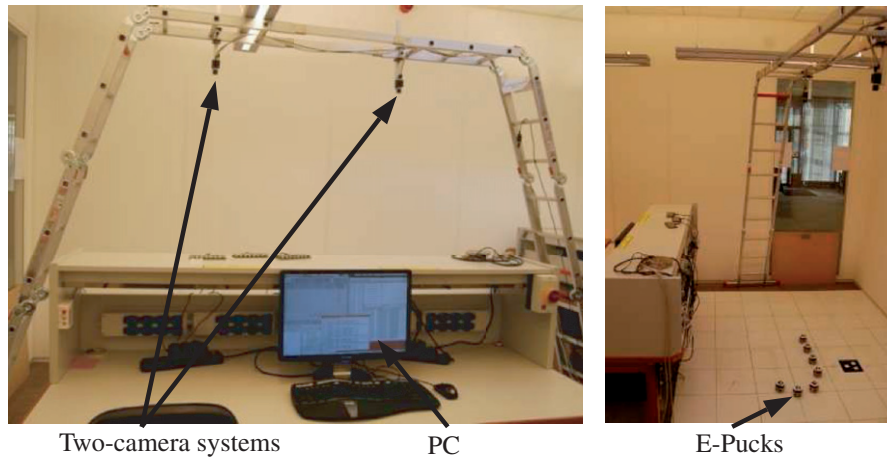


Figure 11. The experimental setup.

5.2 Experimental results

In this section, we illustrate the behaviour of a mobile robot formation under the influence of the kinematic control law given in Theorem 3.1 based on experiments.

The control parameters employed in the experiments are summarised in Table 3. Moreover, the desired virtual structure's trajectory is given by

$$x_{vc}^d(t) = 0.05t - 1.2, \quad (45)$$

$$y_{vc}^d(t) = 0.1 \cos(0.3t) + 0.025t - 0.7, \quad (46)$$

where x_{vc}^d and y_{vc}^d are in meters and t is in seconds.

As in the simulations, the desired formation shape is an equilateral triangle as shown in Figure 4

Table 3. List of control parameters used in experiments in Section 5.2.

$c_i^x = 1_s$	$c_i^y = 30$	$c_i^\phi = 0.5_s$
$\tilde{c}_{ij}^x = 2.5_s$	$\tilde{c}_{ij}^y = 30$	$\tilde{c}_{ij}^\phi = 0.1_s$

where $p_1 = (-0.15 \text{ m}, -\frac{0.15}{\sqrt{3}} \text{ m})^T$, $p_2 = (0.15 \text{ m}, -\frac{0.15}{\sqrt{3}} \text{ m})^T$ and $p_3 = (0 \text{ m}, \frac{0.3}{\sqrt{3}} \text{ m})^T$. Thus the sides of the triangle have a length of 0.3 m. The perturbation is a manual displacement of one of the robots in the formation executed after around 30 s.

The experimental results are presented in Figures 12 and 13. In particular, in Figure 12(a) we present the robots' paths in the case of completely

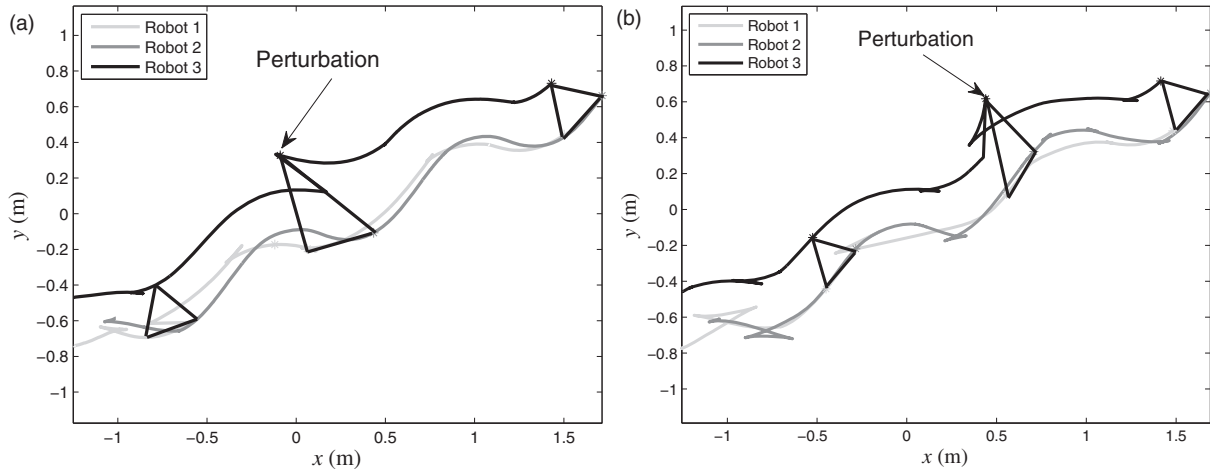


Figure 12. Robot paths obtained in experiments: (a) disconnected communication graph and (b) connected communication graph.

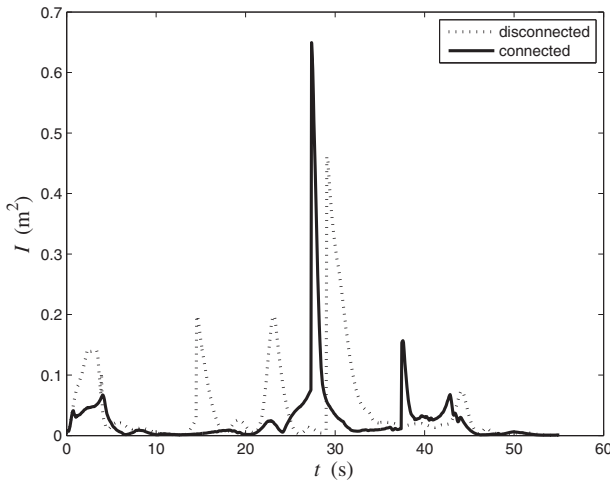


Figure 13. Comparison between formation geometry maintenance index in the case of a connected and a disconnected communication graph.

uncoupled robots, where $\tilde{c}_{ij}^x = 0$, $\tilde{c}_{ij}^y = 0$ and $\tilde{c}_{ij}^\phi = 0$. This is equivalent to a completely disconnected communication graph of the formation. In turn, in Figure 12(b), robots' paths in the plane are presented when the communication graph is connected according to the communication network shown in Figure 3(a). It can be seen in the plots that in both cases robots in the formation converge to the desired formation shape. Moreover, after the perturbation has occurred, the neighbours of the perturbed robot in Figure 12(b) diverge from their desired trajectories to recover the formation shape. This formation keeping behaviour is induced by the coupling terms added to the formation control algorithm and is absent in Figure 12(a) for a

disconnected communication graph. We can therefore again confirm that these additional coupling terms in (16) enhance actual formation behaviour of robots in the formation.

The beneficial influence of allowing robots in the formation to exchange information with each other is also confirmed by examining Figure 13 which compares the formation geometry maintenance index (43) for a connected and a disconnected communication graph. Clearly, when the communication graph is connected, the index is smaller except for the perturbation peak. This is purely due to the fact that in experiments the displacement is done manually and therefore is not equal in the case of a connected and a disconnected communication graph. In fact, it is larger in the experiment with the connected communication graph which may be seen explicitly by comparing Figure 12(a) and (b). Apart from the very moment of the perturbation, the formation geometry maintenance index is smaller for the case of a connected communication graph. Moreover, despite the larger perturbation magnitude, the formation geometry maintenance index decreases faster in the case of a connected communication graph.

6. Conclusions

In this article, a virtual structure controller is designed for the formation control of unicycle mobile robots. We have proposed two controllers depending on the kind of the unicycle robot: one based on a kinematic model of a mobile robot and the other based on a dynamic model of a mobile robot. They both introduce mutual coupling between the individual robots,

thereby providing more robustness to the formation in the face of perturbations as compared to leader-follower (i.e. master-slave) type approaches. Moreover, we give a stability proof of the proposed approach for a formation of an arbitrary number of robots. In doing so, we are able to claim an exponential convergence rate of the formation error variables to zero, which is associated with a certain amount of robustness. Simulations and experiments performed for three-robot systems demonstrate the practical applicability of the approach. These results also show that the tuning of the mutual coupling parameters provides a means to weigh the importance of maintaining formation versus the importance of the individual robots tracking their individual desired trajectories. Moreover, we have observed that if the communication graph of the formation is connected and mutual coupling is effected, the performance of the formation and more specifically sensitivity to perturbations is improved.

Our future work will include a more extensive theoretical analysis of the influence of the connectivity condition of the communication graph on the formation behaviour. Moreover, we want to also examine the case when the persistence of excitation condition does not hold and possibly there are temporary failures in the inter-robot communication.

Acknowledgements

The first author would like to thank to Sisdamanto Adinandra from Eindhoven University of Technology for his kind help in conducting the experiments. Moreover, the travel grant from the Royal Academy of Engineering to support the first author's stay in Eindhoven in 2010 is highly appreciated.

References

- Alvarez Aguirre, A. (2011), 'Remote Control and Motion Coordination of Mobile Robots', PhD thesis, Eindhoven University of Technology, the Netherlands.
- Aneke, E. (2003), 'Control of Underactuated Mechanical Systems', PhD thesis, Eindhoven University of Technology, the Netherlands.
- Arai, T., Pagello, E., and Parker, L.E. (2002), 'Editorial: Advances in Multi-robot Systems', *IEEE Transactions on Robotics and Automation*, 18, 655–661.
- Arkin, R.C. (1998), *Behavior-based Robotics*, London: MIT Press.
- Beard, R.W., Lawton, J., and Hadaegh, F.Y. (2000), 'A Feedback Architecture for Formation Control', in *Proceedings of the American Control Conference*, Vol. 6, pp. 4087–4091.
- Bicho, E., and Monteiro, S. (2003), 'Formation Control for Multiple Mobile Robots: A Nonlinear Attractor Dynamics Approach', in *IEEE/RSJ International Conference on Intelligent Robots and Systems*, Vol. 2, pp. 2016–2022.
- Bishop, R. (2005), *Intelligent Vehicle Technology and Trends*, Norwood: Artech House.
- Burgard, W., Moors, M., Stachniss, C., and Schneider, F. (2005), 'Coordinated Multi-robot Exploration', *IEEE Transactions on Robotics*, 21, 376–386.
- Carelli, R., de la Cruz, C., and Roberti, F. (2006), 'Centralized Formation Control of Nonholonomic Mobile Robots', *Latin American Applied Research*, 36, 63–69.
- Chen, Y.Q., and Wang, Z. (2005), 'Formation Control: A Review and a New Consideration', in *Proceedings of the IEEE/RSJ International Conference on Intelligent Robots and Systems*, pp. 3181–3186.
- Consolini, L., Morbidi, F., Prattichizzo, D., and Tosques, M. (2006), 'On the Control of a Leader-follower Formation of Nonholonomic Mobile Robots', in *IEEE Conference on Decision and Control*, pp. 5992–5997.
- Desai, J.P., Ostrowski, J.P., and Kumar, V. (2001), 'Modeling and Control of Formations of Nonholonomic Mobile Robots', *IEEE Transactions on Robotics and Automation*, 17, 905–908.
- Do, K., and Pan, J. (2007), 'Nonlinear Formation Control of Unicycle-type Mobile Robots', *Robotics and Autonomous Systems*, 55, 191–204.
- Durrant-Whyte, H., and Bailey, T. (2006), 'Simultaneous Localization and Mapping: Part I', *IEEE Robotics and Automation Magazine*, 13, 99–108.
- Fliess, M., Lévine, J., Martin, P., and Rouchon, P. (1995), 'Flatness and Defect of Non-linear Systems: Introductory Theory and Examples', *International Journal of Control*, 61, 1327–1361.
- Godsil, C., and Royle, G. (2001), *Algebraic Graph Theory*, New York: Springer.
- Horn, R.A., and Johnson, C.R. (1990), *Matrix Analysis*, New York: Cambridge University Press.
- Ikeda, T., Jongusuk, J., Ikeda, T., and Mita, T. (2006), 'Formation Control of Multiple Nonholonomic Mobile Robots', *Electrical Engineering in Japan*, 157, 81–88.
- Ioannou, P.A., and Sun, J. (1995), *Robust Adaptive Control*, Upper Saddle River, NJ: Prentice-Hall.
- Jakubiak, J., Lefeber, E., Tchoń, K., and Nijmeijer, H. (2002), 'Two Observer-based Tracking Algorithms for a Unicycle Mobile Robot', *International Journal of Applied Mathematical and Computer Science*, 12, 513–522.
- Jiang, Z.P., and Nijmeijer, H. (1997), 'Tracking Control of Mobile Robots: A Case Study in Backstepping', *Automatica*, 33, 1393–1399.
- Kanayama, Y., Kimura, Y., Miyazaki, F., and Noguchi, T. (1990), 'A Stable Tracking Control Method for an Autonomous Mobile Robot', in *Proceedings of the IEEE International Conference on Robotic Automata*, pp. 384–389.
- Khalil, H.K. (1996), *Nonlinear Systems* (2nd ed.), Upper Saddle River, NJ: Prentice Hall.
- Kitano, H., Asada, M., Kuniyoshi, Y., Noda, I., Osawa, E., and Matsubara, H. (1997), 'RoboCup: A Challenge Problem for AI', *AI Magazine*, 18, 73–85.
- Kolmanovsky, I., and McClamroch, N.H. (1995), 'Developments in Nonholonomic Control Problems', *IEEE Control Systems Magazine*, 15, 20–36.

- Kostić, D., Adinandra, S., Caarls, J., and Nijmeijer, H. (2010), 'Collision-free Motion Coordination of Unicycle Multi-agent Systems', in *American Control Conference (ACC)*, pp. 3186–3191.
- Laumond, J. (ed.) (1998), *Robot Motion Planning and Control* (Vol. 229), Berlin/Heidelberg: Springer.
- Lefeber, A.A.J. (2000), 'Tracking Control of Nonlinear Mechanical Systems', PhD thesis, University of Twente, the Netherlands.
- Leonard, N.E., and Fiorelli, E. (2001), 'Virtual Leaders, Artificial Potentials and Coordinated Control of Groups', in *Proceedings of the 40th IEEE Conference Decision and Control*, Vol. 3, pp. 2968–2973.
- Lewis, M.A., and Tan, K.H. (1997), 'High Precision Formation Control of Mobile Robots using Virtual Structures', *Autonomous Robots*, 4, 387–403.
- Mondada F., and Bonani, M. (2007), 'E-Puck Education Robot', <http://www.e-puck.org/>
- Morin, P., and Samson, C. (2008), 'Motion Control of Wheeled Mobile Robots', in *Springer Handbook of Robotics*, eds. B. Siciliano, and O. Khatib, Berlin, Heidelberg: Springer, pp. 799–826.
- Narendra, K.S., and Annaswamy, A.M. (1989), *Stable Adaptive Systems*, Englewood Cliffs, NJ: Prentice Hall.
- Panteley, E., Lefeber, E., Loria, A., and Nijmeijer, H. (1998), 'Exponential Tracking Control of a Mobile Car using a Cascaded Approach', in *Proceedings IFAC Workshop on Motion Control*, pp. 221–226.
- Panteley, E., and Loria, A. (1998), 'On Global Uniform Asymptotic Stability of Nonlinear Timevarying Systems in Cascade', *Systems and Control Letters*, 33, 131–138.
- Parker, L.E. (2008), 'Multiple Mobile Robot Systems', in *Springer Handbook of Robotics*, eds. B. Siciliano, and O. Khatib, Berlin, Heidelberg: Springer, pp. 921–941.
- Rodriguez-Angeles, A., and Nijmeijer, H. (2003), *Synchronization of Mechanical Systems*, Singapore: World Scientific.
- Rodriguez-Angeles, A., and Nijmeijer, H. (2004), 'Mutual Synchronization of Robots via Estimated State Feedback: A Cooperative Approach', *IEEE Transactions on Control Systems Technology*, 12, 542–554.
- Rugh, W.J. (1993), *Linear System Theory*, Englewood Cliffs, NJ: Prentice-Hall.
- Sørdalen, O., and Egeland, O. (1995), 'Exponential Stabilisation of Nonholonomic Chained Systems', *IEEE Transactions on Automatic Control*, 40, 35–49.
- Takahashi, H., Nishi, H., and Ohnishi, K. (2004), 'Autonomous Decentralised Control for Formation of Multiple Mobile Robots Considering Ability of Robot', *IEEE Transactions on Industrial Electronics*, 51, 1272–1279.
- Tanner, H.G., Pappas, G.J., and Kumar, V. (2004), 'Leader-to-Formation Stability', *IEEE Transactions on Robotics and Automation*, 20, 443–455.
- van den Broek, T., van de Wouw, N., and Nijmeijer, H. (2009), 'Formation Control of Unicycle Mobile Robots: A Virtual Structure Approach', in *Proceedings of the IEEE Conference on Decision and Control*, pp. 8328–8333.
- Vidal, R., Shakernia, O., and Sastry, S. (2003), 'Formation Control of Nonholonomic Mobile Robots with Omnidirectional Visual Servoing and Motion Segmentation', *IEEE International Conference on Robotics and Automation*, 1, 584–589.
- Wang, Z., Takano, Y., Hirata, Y., and Kosuge, K. (2007), 'Decentralised Cooperative Object Transportation by Multiple Mobile Robots with a Pushing Leader', in *Distributed Autonomous Robotic Systems*, eds. R. Alami, R. Chatila, and H. Asama, Vol. 6, Japan: Springer, pp. 453–462.
- Yamaguchi, H. (1999), 'A Cooperative Hunting Behavior by Mobile-robot Troops', *International Journal of Robotics Research*, 18, 931–940.
- Yanakiev, D., and Kanellakopoulos, I. (1996), 'A Simplified Framework for String Stability Analysis in AHS', in *Preprints of the 13th IFAC World Congress*, pp. 177–182.
- Yoshioka, C., and Namerikawa, T. (2008), 'Formation Control of Nonholonomic Multi-vehicle Systems Based on Virtual Structure', in *Proceedings of the 17th IFAC World Congress*, Seoul, Korea, pp. 5149–5154.
- Young, B.J., Beard, R.W., and Kelsey, J.M. (2001), 'A Control Scheme for Improving Multivehicle Formation Maneuvers', in *Proceedings of the American Control Conference*, Arlington, VA, USA, pp. 704–709.